ORIGINAL RESEARCH **Open access**

Data-Driven Prioritization of Residential Energy Efficiency Measures for Cost-Effective Community Savings

George Wilson[1*], Chloe Bennett[2], Jack Turner[1]

Abstract

Numerous US utility companies promote residential energy conservation via rebate programs, frequently reacting to state-level energy reduction requirements or the strategic goal of lowering demand to avoid expanding generation infrastructure. A core presumption of these incentive initiatives is that the most energy-inefficient homes are the most likely to use these rebates; however, this paradigm does not always hold. The primary objective of this research was to assess the viability of prioritized incentivization—specifically, ranking incentives to maximize energy conserved per dollar invested across an entire municipality. This investigation employs a data mining methodology that utilizes established structural and energy attributes to forecast the power usage of homes, which together serve as a representative sample of all dwellings within a given community. Using this model, the study calculates natural gas usage, potential savings, and the associated implementation costs of implementing the most effective energy conservation strategies. These projected savings and expenditures enable the creation of a phased energy mitigation strategy, targeting the most economically advantageous interventions throughout the entire utility service area. Findings indicate that a 36% reduction in energy usage is attainable at a levelized expense of under $14 per mmBTU ($14,780 per MJ), illustrating the robust efficacy of this methodology. A parallel Economic Input–Output Analysis delineates the ripple effects this strategy has on the local economy. The analysis reveals that across approximately 45,000 single-family homes in the examined area, a preliminary $26M expenditure on energy efficiency could generate an aggregate multiplier economic effect of $41M, alongside supplementary economic benefits of $2.2M over the lifespan of the evaluated efficiency improvements.

Keywords Machine learning, Building energy efficiency, Data mining, Levelized cost of energy saving, Energy reduction strategy, Economic input–output analysis

*Correspondence:
George Wilson
g.wilson@leeds.ac.uk
[1] Department of Intelligent Electrical Networks, Faculty of Engineering, University of Leeds, Leeds, United Kingdom
[2] Department of Machine Learning for Energy Systems, Faculty of Engineering, University of Sheffield, Sheffield, United Kingdom

Introduction

In 2015, the United States building sector accounted for 45% of the nation's CO2 emissions [1]. There is an established target to decrease energy consumption in both residential and commercial building domains by at least 35% before 2030 [2]. In recent times, focusing on community-wide building energy conservation has garnered substantial interest, as it offers distinct avenues to accomplish energy efficiency and integrate renewable energy sources from various standpoints [3-9]. Several prior investigations have explored community-level trajectories for curtailing energy usage [10-15]. While these analyses demonstrated that behavioral modifications, minimized air infiltration, combined insulation and infiltration

This is an open access article distributed under the terms of the Creative Commons Attribution-NonCommercial-ShareAlike 4.0 International License (CC BY-NC-SA 4.0), which permits non-commercial use, distribution, reproduction, and adaptation in any medium or format, provided that appropriate credit is given to the original author(s) and source, a link to the license is provided, and any changes made are indicated. Adapted material must be distributed under the same license.

© 2026 The Author(s). | Published by Institute of Smart Energy Systems Press

strategies, and extensive retrofitting yielded prospective energy conservation, their projections relied on generalized presumptions concerning residential energy profiles. One investigation assessed multiple Energy Efficiency (EE) frameworks designed to enhance EE, noting fluctuating levels of uniformity in their execution and success. This research determined that demand-side administration could generate annual energy savings of 4 quads and a carbon mitigation of 63 million metric tons per year [16]. Koomey *et al*. [17] leveraged building sector data from diverse repositories to formulate policy models aimed at augmenting EE, projecting that a rigorous EE initiative could produce energy conservation and carbon emission reductions of 20% and 40%, respectively, by the year 2025.

Contemporary research has predicted building thermal and cooling requirements through the application of data mining methodologies [18-22]. Neural networks (NN) are extensively employed to project the energy consumption of structures [23]. Findings indicated that while solar radiation and ambient temperature exerted a profound influence, other variables could be excluded from the forecasting models. Certain analyses have integrated Bayesian NN approaches to evaluate building energy utilization, incorporating standard environmental variables as inputs [24-28]. Artificial neural network (ANN) systems were applied to predict the energy performance of residential structures, utilizing diverse environmental attributes as input factors and overall energy expenditure as the output metric [29]. **Table 1**, presented below, catalogs antecedent efforts by researchers who applied machine learning methodologies to forecast residential energy utilization. This tabular summary details the respective researchers, the specific techniques employed, the predictive variables used, the targeted consumption metrics, and the accuracy of the resulting forecasts.

Table 1. Document of prior research in predicting energy consumption in residential buildings.

Study/Prediction method	Building/Energy system characteristics	Input variables	Target variable	Prediction output	Performance metric
(Aqlan *et al*., 2014)/Artificial Neural Network (ANN) with cluster analysis	Not specified	Dry-bulb temperature, relative humidity, and solar irradiance	Annual energy demand	Annual energy consumption	Root Mean Square Error (RMSE) = 0.031
(Chae *et al*., 2015)/Artificial Neural Network (ANN)	Commercial buildings with HVAC temperature set-point schedules	Day-type classification, time of day, outdoor dry-bulb temperature, and outdoor humidity	Historical energy-use records and hour of the day	Electricity consumption at 15-minute intervals and daily peak electricity demand	Coefficient of determination (R^2) = 0.902; Coefficient of Variation (CV) = 8.5%
(Karatasou *et al*., 2005)/Artificial Neural Network (ANN)	Not specified	Ambient temperature, solar radiation, relative humidity, and wind speed	Building load demand	Hourly building energy loads	Mean Bias Error (MBE) = 0.13
(González-Vidal *et al*., 2016)/Bayesian Regularized Neural Networks and Random Forest	Not specified	Historical hourly data including outdoor temperature, humidity (%), solar irradiance, wind speed, wind	Daily energy-use data	Daily energy consumption forecasting	Coefficient of determination (R^2) for both methods ranged from 0.65 to 0.75

© 2026 The Author(s). | Published by Institute of Smart Energy Systems Press

		direction, dew point temperature, and vapor-pressure deficit			
(Fan *et al.*, 2014)/Eight widely used forecasting algorithms	Not specified	Commercial-building energy consumption records and meteorological information	Building power-consumption data collected at 15-minute intervals	Next-day energy consumption and peak power demand prediction	Mean Absolute Percentage Error (MAPE): 2.32% for next-day energy consumption and 2.85% for peak power demand

Enhancing the economic efficiency of utility-sponsored energy reduction initiatives by directing rebate funds toward homes with the highest potential for savings has been the primary motivation behind several recent studies. An evaluation of the financial advantages of EE enhancements for dwellings in the Desert region was conducted utilizing discrete building energy simulations to forecast the yearly electrical conservation and return-on-investment timelines for multiple upgrades, facilitating the creation of a financially viable EE rebate strategy [30]. A comparable investigation [31] leveraged accessible residential structural information alongside historical energy metrics for homes in a US Midwestern locale to pinpoint properties poised to generate maximum savings from distinct interventions; nonetheless, their evaluations relied upon somewhat debatable premises. For instance, the researchers posited that elevated weather-normalized heating energy consumption in a given home correlated with uniformly inadequate wall and attic insulation, subpar window thermal performance, and inefficient heating systems. In practice, however, the energy efficiency of these distinct architectural elements is often not homogeneous. The complete lack of attic insulation, as an example, could act as the nearly exclusive cause for a dwelling's excessive energy utilization.

The financial advantages of EE extend beyond the monetary savings realized by individual homeowners, encompassing broader community impacts such as employment generation and augmented local disposable income. Along these lines, one investigation established a methodical architecture to measure the municipality-wide repercussions of residential EE expenditures [32]. Using an Economic Input–Output Analysis focused on Montgomery County, Ohio, the authors found that a $14M capital injection into residential heating, ventilation, and air conditioning (HVAC) systems could generate an aggregate economic ripple effect of $22M. Briefly, a machine learning paradigm is deployed to construct a unified model capable of predicting the thermal requirements across diverse residential properties. The outcomes revealed that the projected conservation aligned with the realized savings to within a 2.5% margin for the majority of the energy efficiency strategies evaluated in the research.

Materials and Methods

Figure 1 illustrates the operational framework implemented in this investigation. Initially, information was gathered to forecast the power requirements of individual residences. The subsequent phase involved computing deduced energy attributes derived from longitudinal monthly natural gas consumption and meteorological records. The third procedure aimed to isolate the variables exerting the most substantial influence on energy utilization by applying a Random Forest (RF) algorithm. The fourth operation focused on formulating a singular NN architecture to predict the energy consumption metrics for every dwelling. In the fifth stage, both singular and aggregated energy conservation potentials were calculated. The sixth phase sought to corroborate the anticipated savings utilizing a k-nearest neighbors (KNN) computational method. The seventh process estimated the most economically viable energy enhancement alternatives by deploying a "worst-to-first" prioritization scheme. The final step quantified the broader municipal economic consequences

© 2026 The Author(s). | Published by Institute of Smart Energy Systems Press

stemming from the strategic energy efficiency capital allocations derived from the study's findings. The subsequent sub-sections elaborate on the intricacies of each phase of the research.

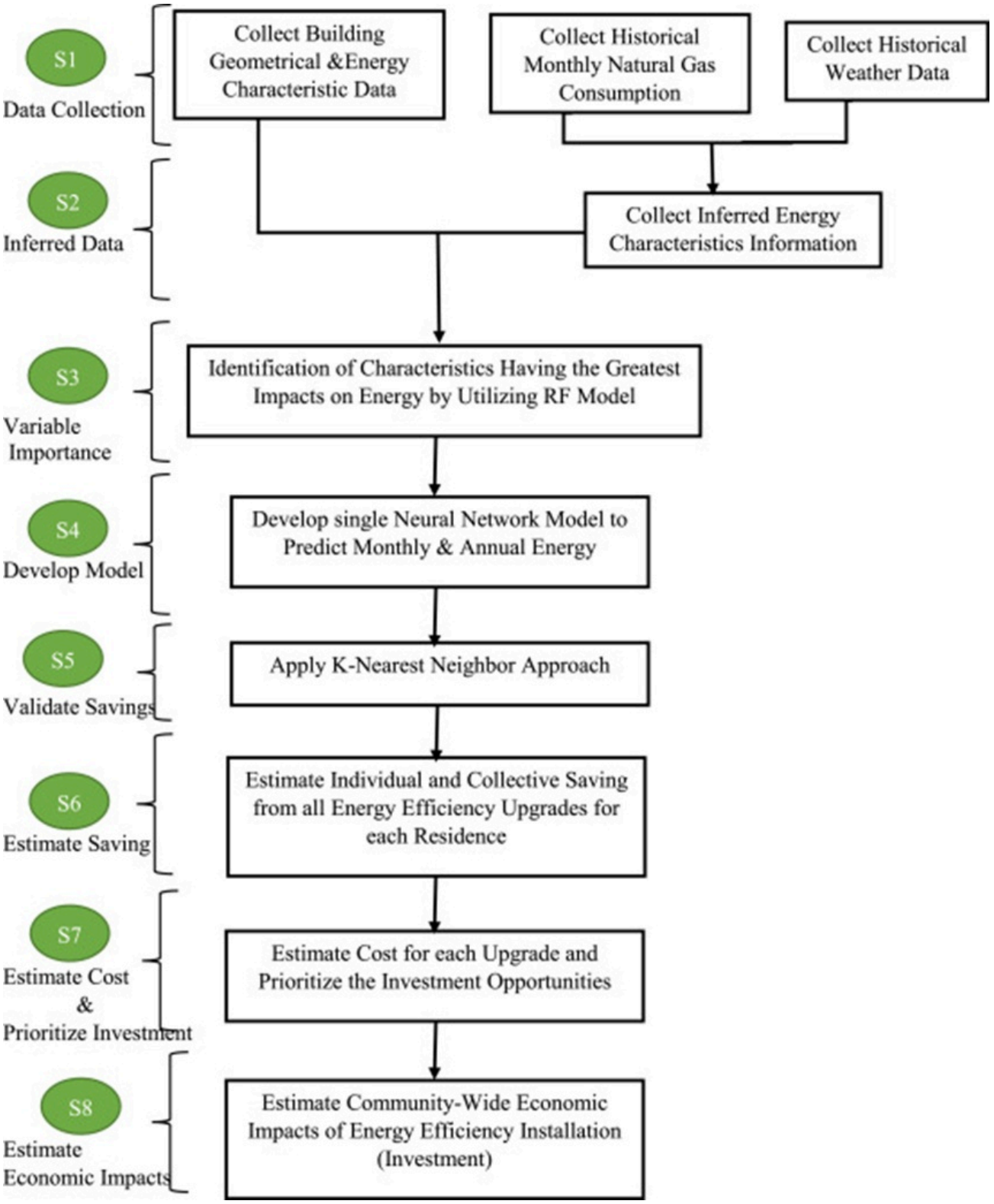

Figure 1. Eight research steps of proposed framework.

© 2026 The Author(s). | Published by Institute of Smart Energy Systems Press

Data and information collection (Steps 1 and 2)

This study was facilitated by access to an aggregate cluster of more than 500 residential structures utilized as student accommodations, which are the property of a university in the Midwestern US. These dwellings exhibited considerable diversity regarding dimensions (ranging from 66 to 258 square meters of floor space), construction age (spanning from almost 100 years to merely 2 years), and energy efficiency. The variance in energy performance primarily stemmed from incremental renovations executed on the properties over the preceding fifteen years. The dataset compiled for this analysis encompassed the accessible historical monthly electrical and natural gas consumption records for these properties. Furthermore, during the summer of 2015, the academic institution executed energy audits across 139 of these dwellings, which recorded details concerning building envelope insulation, window specifications, resident occupancy, kitchen appliances, HVAC systems, domestic hot water infrastructure, and the presence or type of basements. Lastly, real estate documentation from the county auditor supplied comprehensive structural data for every dwelling. **Table 2** displays the maximum and minimum parameters of the architectural data. For example, the empirically assessed wall thermal resistance, Rwall, ranged from 0.7 to 2.43 m2K/W; the attic thermal resistance, Rattic, varied between 1.14 and 7.1 m2K/W; and furnace efficiency levels fluctuated between 60% and 95%.

Table 2. Residential house characteristics achieved from the energy audit.

Characteristics	Max	Min
A_{floor} (m^2)	258	66
A_{wall} (m^2)	302	54
A_{window} (m^2)	27	7
A_{attic} (m^2)	245	43
Attic penetration area (cm^2)	3716	None
Basement duct vent area (cm^2)	348	None
R_{attic} (m^2K/W)	7.1	1.14
R_{window} (m^2K/W)	0.35	0.18
R_{wall} (m^2K/W)	2.43	0.70
$R_{basement}$ (m^2K/W)	0.88	0.70
Occupants (number)	12	2
Efficiency of furnace (%)	95	60
Water heater (energy factor)	0.96	0.55
Seasonal energy efficiency ratio (SEER (AC))	16	None

Figure 2 depicts the extent of variability within the recorded geometrical attributes of the structures, revealing substantial fluctuations across the floor, wall, window, and attic spaces of the residences.

© 2026 The Author(s). | Published by Institute of Smart Energy Systems Press

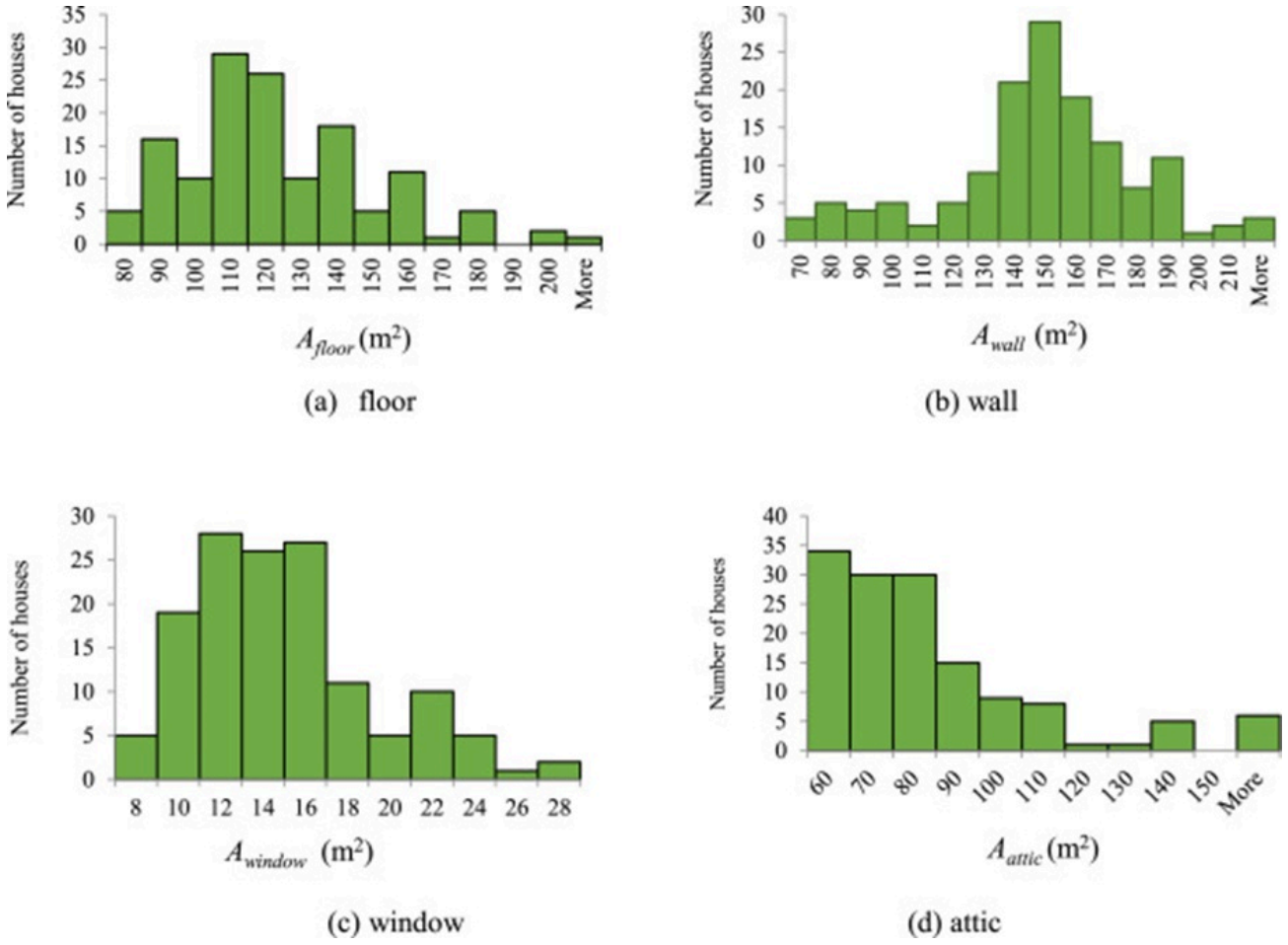

Figure 2. Histograms showing the variation of the building characteristics.

Figure 3 displays the variability among distinct energy parameters, including Rattic, Rwindow, and Rwall, alongside the efficiency of the furnace heating apparatus, water heating unit, and AC SEER rating. Evidently, except for Rwindow **(Figure 3b)**, every characteristic exhibited marked variance.

© 2026 The Author(s). | Published by Institute of Smart Energy Systems Press

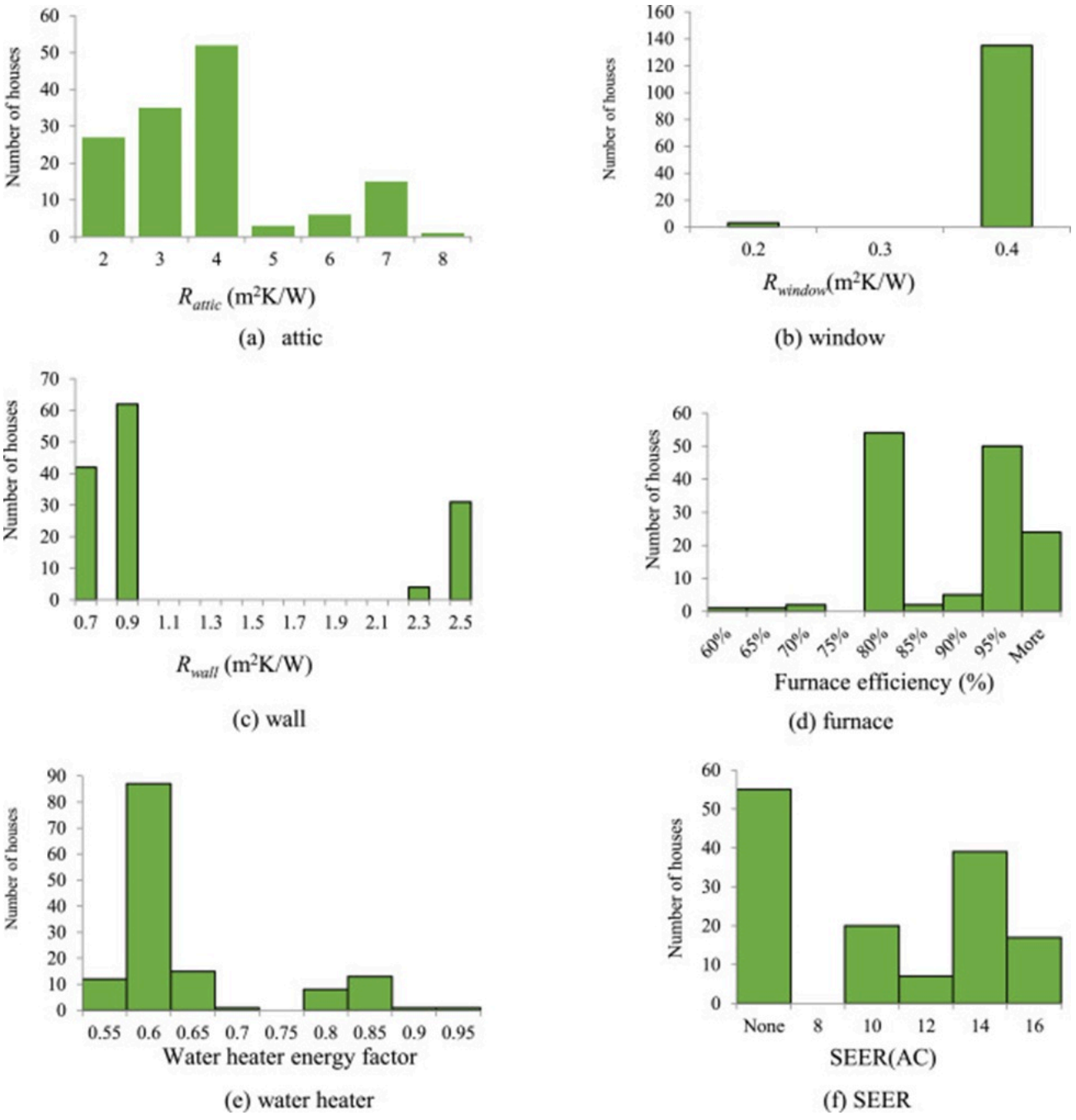

Figure 3. Histograms for the effectiveness of energy efficiency measures.

Identification of characteristics (Step 3)

A random forest algorithm is employed to pinpoint specific geometric and energetic traits of the buildings (acting as predictor variables), aiming to determine the most relevant structural elements for incorporation into the neural network (NN) framework. This methodology was initially introduced in a previous investigation [33] addressing both regression and classification challenges. The formulated random forest model integrated the input Ai/Ri, wherein Ai and Ri represent the surface area and thermal resistance of the building envelope components, respectively. While infiltration rates might be measured through blower door assessments for every evaluated home, acquiring these metrics on a large scale would be

© 2026 The Author(s). | Published by Institute of Smart Energy Systems Press

financially prohibitive and logistically impractical. Consequently, the current investigation incorporates those structural predictors attainable through standard post-construction property evaluations, routine real estate transactions, and accessible longitudinal energy records for each dwelling.

Moreover, to maximize the utility of existing energy metrics for forecasting the natural gas utilization of individual homes, and recognizing the robust performance of regression models correlating energy to temperature within NN frameworks, this research evaluated three supplementary attributes as potential predictive variables. These encompass the heating slope, HSgas (W/K); the weather-independent gas intensity E_(baseline, gas, i) (MJ/m2); the heating temperature balance point temperature, Tbalh, gas (°C), which denotes the mean thermal threshold below which artificial heating is initiated; and the weather-independent electric intensity, E_(baseline, electric), (kWh/m2). These natural gas metrics were derived utilizing a three-parameter regression technique (the Prism method) [34], aligning the monthly gas utilization (MJ/month) with the mean external temperature T_outside (°C) throughout the measurement duration. Here, the variable H represents the Heaviside function, as delineated in **Eq. 1.**

$$E_{i,gas} = E_{baseline,gas,i} + HS_{gas}\left(T_{balh,gas} - T_{outside}\right)\mathrm{H}\left(T_{balh,gas} - T_{outside}\right) \quad (1)$$

The electrical metric, $E_{baseline,electric}$, along with the cooling slope ⟦ CS_{elec} (Wh/K), were generated through an analogous three-parameter regression analyzing monthly electrical use against the mean monthly external temperature [34], structured as follows:

$$E_{i,electric} = E_{baseline,electric,i} + CS_{elec}\left(T_{outside} - T_{balc}\right) \quad (2)$$

A fundamental premise here is that weather-independent electrical utilization introduces supplementary thermal energy into a structure, thereby exerting a measurable influence on the overall natural gas demand. The energetic consumption variables evaluated within the random forest algorithm are detailed in **Table 3,** which delineates the relative significance of every predictor in forecasting energy use.

Table 3. Predictors for gas consumption ranked by influence on energy consumption.

Order of variable importance (most to least important)	Predictors
1	Heating slope, HS_{gas} (W/K)
2	Wall area/R_{wall} (W/m^{2}K)
3	Baseline electric intensity ($Baseline_e$) (kWh/m^2)
4	$T_{balh,gas}$ (°C)
5	Furnace efficiency () (%)
6	Attic area/R_{attic} (W/m^{2}K)
7	Floor area (m^2)
8	Window area/R_{win} (W/m^{2}K)
9	Energy factor for water heater (EF, WH)
10	Maximum occupancy

© 2026 The Author(s). | Published by Institute of Smart Energy Systems Press

11	Attic penetration area (cm^2)
12	Basement duct vent area (cm^2)
13	Basement duct vent open
14	$R_{basement}$ (m^2 K/W)

Figure 4 illustrates the natural gas usage predictors, ordered according to their impact on overall energy utilization. The findings indicate that the gas heating slope exerted the most substantial effect on energy demand (evidenced by a greater magnitude). In contrast, factors such as attic penetration area, Rbasement, and the state of basement duct vents demonstrated a weaker correlation with energy use (lower magnitude). Consequently, these less impactful variables were excluded from the neural network framework detailed in the subsequent section.

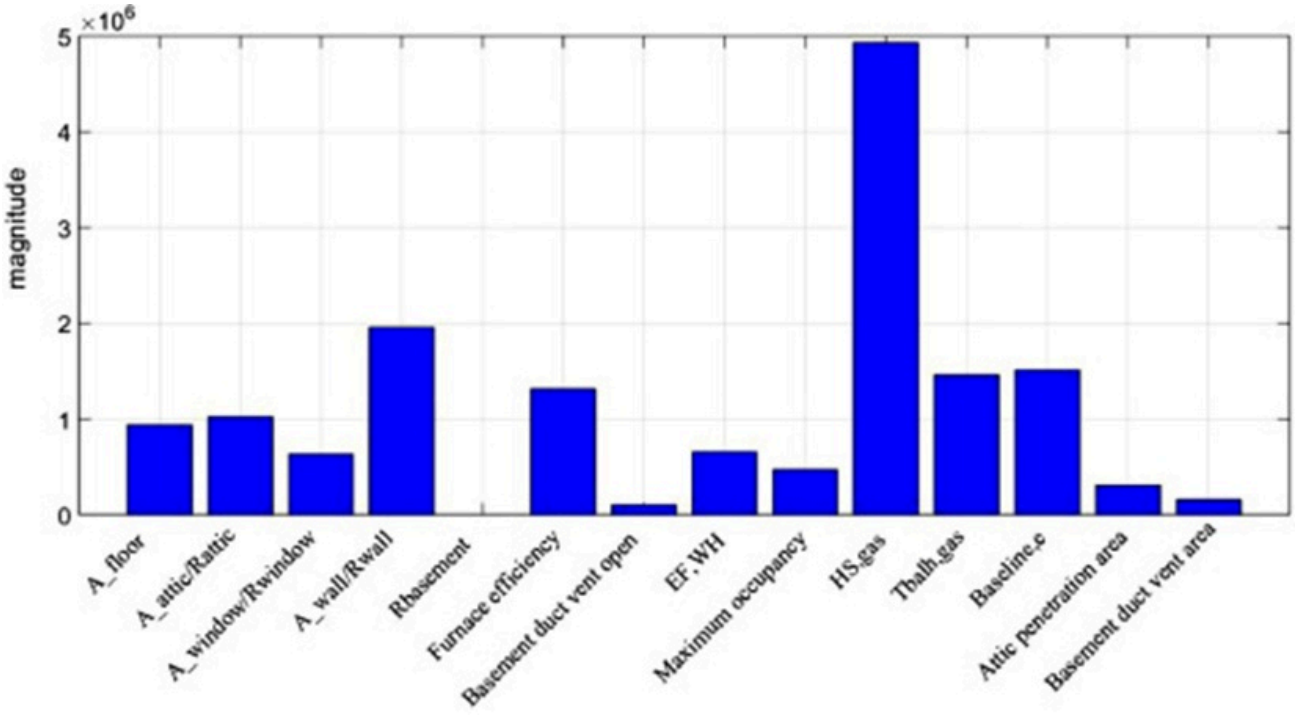

Figure 4. The variable importance shown by the random forest approach.

Develop neural network model (Step 4)

Artificial neural networks (ANN) are widely implemented across diverse energy modeling contexts. The primary benefit of employing an ANN lies in its capacity to process nonlinear dynamics [35]. The current research deployed a feed-forward ANN architecture to correlate energy consumption with the geometric dimensions and thermal attributes of residential dwellings identified as highly significant. The objective was to create a single, generalized ANN framework capable of forecasting natural gas utilization for any given residence, rather than generating distinct models for each specific property. **Table 4** itemizes the input variables determined to hold the highest predictive value for energy consumption, as derived from the random forest analysis, and also specifies the targeted output metric. In total, the dataset comprised 11 distinct data features that served as inputs.

Table 4. The data used in ANN model construction.

© 2026 The Author(s). | Published by Institute of Smart Energy Systems Press

Parameter	Model input	Model output
A_{window} /R_{window} (W/K)	X	
A_{wall} /R_{wall} (W/K)	X	
Furnace efficiency (%)	X	
Wall thermal conductance, (A_{wall}/R_{wall}) (W/K)	X	
Furnace efficiency, (\eta_{fur}) (%)	X	
Water heater energy factor	X	
Base electrical energy intensity (kWh/m²)	X	
Occupancy count (number of residents)	X	
Gas heating slope, (HS_{gas}) (W/K)	X	
Heating balance-point temperature (°C)	X	
Mean monthly outdoor air temperature (°C)	X	
Monthly natural gas consumption (MJ/month)		X

Table 5 displays comparative data between two distinct residences. The informational samples were segregated into dual classifications: one representing the heating period (spanning October to April) and another encompassing the remainder of the annual cycle. The heating season grouping, serving as the central focus of this investigation, contained an aggregate of 973 samples.

Table 5. Example of data inputs for ANN model construction.

Parameter	*House Sample #1*				*House Sample #2*			
	Oct.	Nov.	…	Apr.	Oct.	Nov.	…	Apr.
A_{floor} (m²)	104	104	…	104	124	124	…	124
A_{attic} /R_{attic} (W/K)	23	23	…	23	42	42	…	42
A_{window} /R_{window} (W/K)	53	53	…	53	50	50	…	50
A_{wall} /R_{wall} (W/K)	192	192	…	192	174	174	…	174
Furnace efficiency, (%)	95	95	…	95	70	70	…	70
Water-heater energy factor	0.55	0.55	…	0.55	0.63	0.63	…	0.63
Baseline electricity intensity (kWh/m)	65.88	65.88	…	65.88	60.81	60.81	…	60.81
Occupancy level (number of residents)	6	6	…	6	5	5	…	5
Heating slope, HS_{gas} (W/K)	3.77	3.77	…	3.77	3.77	3.77	…	3.77
Heating balance-point temperature (°C)	14.72	14.72	…	14.72	19.63	19.63	…	19.63
Mean monthly outdoor temperature (°C)	10.67	4.97	…	10.67	10.67	4.97	…	10.96

© 2026 The Author(s). | Published by Institute of Smart Energy Systems Press

Output: Monthly natural gas consumption (MJ/month)	5811	13,34	…	16,68	5811	17,75	…	19,90

The established deep learning ANN framework consists of a networked array of nodes, bridging input and output layers via intermediate hidden nodes. Every individual node executes a mathematical operation to convert incoming data into a modified output signal. The numerical weights assigned to these network linkages are autonomously adjusted to reduce the discrepancy between projected outcomes and empirical targets. During model development, 70% of the dataset was allocated for training, 15% was reserved for testing, and the remaining 15% was used for validation. The optimal outcomes, characterized by the highest correlation coefficient (R2), were achieved using a comparatively straightforward neural architecture containing dual hidden layers (each possessing 11 nodes) alongside a tanh activation function.

To evaluate the statistical validity of the forecasted values, a paired-samples t-test was executed to contrast the projected aggregate gas usage against the empirically recorded gas consumption. The established null hypothesis for this assessment posited that the mean values of the observed and modeled datasets were dissimilar. The t-test outcomes, presented in **Table 6**, demonstrate no statistically significant variation between the paired data sequences. This analytical review confirms that the statistical means of both arrays were highly comparable; furthermore, the resulting probability score of 0.921 signifies a lack of meaningful divergence between the two sets at the predetermined 0.05 level of significance.

Table 6. Two-sample t-tests for actual vs. predicted.

Data category	Number of samples	Average value	Standard deviation	Standard error of the mean	95% confidence interval for the difference	Estimated difference	t-statistic	P-value
Measured values	139	1206	383	32	(−85.53, 94.63)	4.54	0.1	0.921
Forecasted values	139	1202	380	32	—	—	—	—

The computational model formulated in this investigation demonstrated a robust capacity to project natural gas demand. **Figure 5** illustrates a specific set of findings regarding the prediction of yearly thermal energy use across a residential sample group. Within this visualization, the empirically recorded consumption (blue) is juxtaposed against the forecasted usage (orange) for every respective home.

© 2026 The Author(s). | Published by Institute of Smart Energy Systems Press

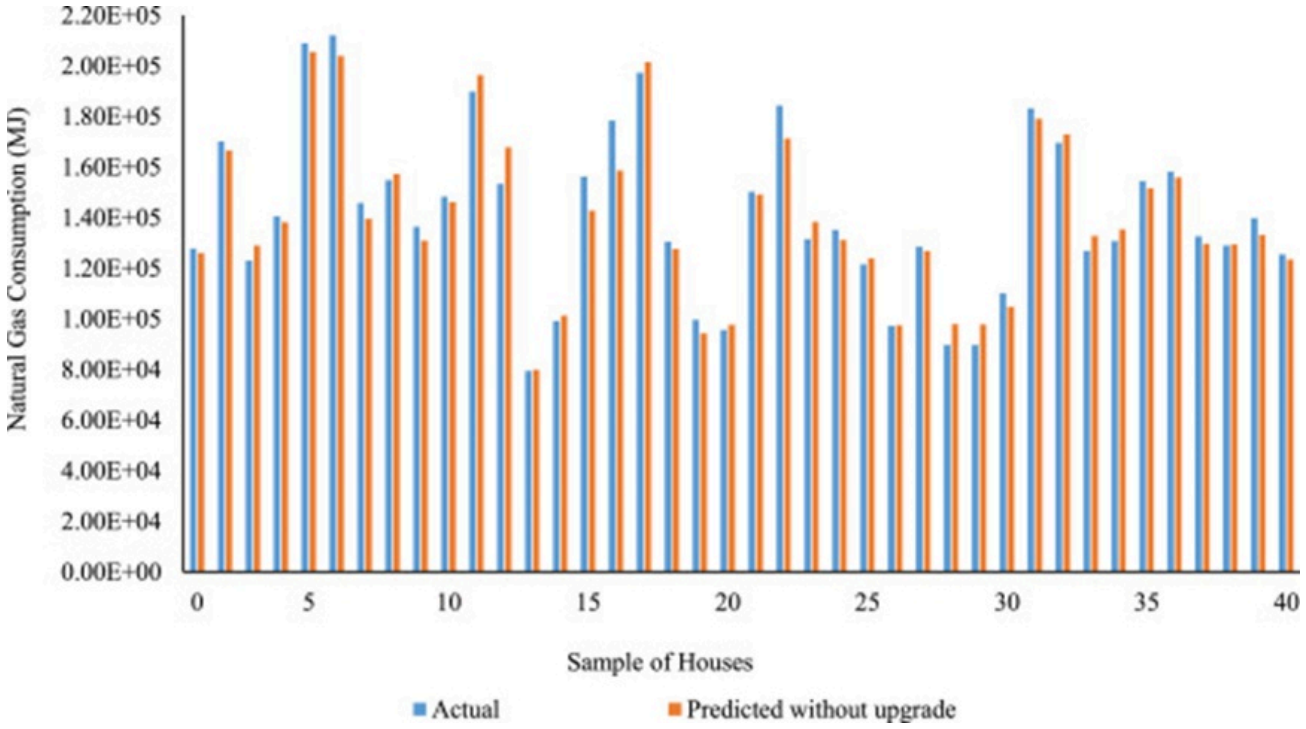

Figure 5. Actual and predicted annual natural gas consumption for a random sampling of houses for the October 1–April 1 study period.

Applying K-nearest neighbor approach (Step 5)

As highlighted in the preceding segments, the thermal performance attributes of the evaluated dwellings exhibit broad variability. While certain properties underwent renovations across various timeframes, distinct pre- and post-retrofit metrics were unrecorded for discrete dwellings. Consequently, a “nearest neighbor” methodology was deployed to corroborate the energy reductions linked to these enhancements [36]. This analytical technique isolates the highest-probability upgraded dwelling within the broader housing clusters. Specifically, a K-nearest neighbor algorithm served to verify the conservation outcomes across six sample properties. To measure the proximity or ‘closeness’ between a modified dwelling and an unmodified counterpart, researchers utilized a Euclidean squared distance parameter—calculated as the sum of the squared discrepancies between the traits of the analyzed home and its closest matching peer. This differential error is formally expressed as:

$$Error = \sum_{j}^{n} \left(f_{u,j} - f_{c,j} \right)^2 \quad (3)$$

Where n is the number of inputs, fu,j is upgraded energy characteristics, and fc,j is current energy characteristics.

Within **Figure 6**, six target dwellings slated for renovations are evaluated to substantiate potential conservation outcomes by benchmarking them against properties that already possess augmented thermal profiles. Following the theoretical application of distinct interventions—such as enhanced window systems and supplemental attic or wall insulation—the subsequent power demands of these homes were verified. This was achieved by juxtaposing the algorithmically forecasted post-retrofit energy usage against the empirical consumption of the corresponding nearest neighbor property. The primary variables leveraged to establish these nearest neighbor pairings consisted of the most critical structural and

© 2026 The Author(s). | Published by Institute of Smart Energy Systems Press

empirical energy predictors identified by the ANN framework: specifically, A_{floor}; A_{wall}; A_{window}; A_{attic}; R_{attic}; R_{window}; R_{wall}; # of occupants; water heater EF; heating system efficiency. Correlating the ANN's projected post-intervention energy utilization with the authentic usage of the post-upgrade K-nearest neighbor revealed highly consistent alignments between the neural network's forecasts and the actual operational demands of the matched homes. Because the Euclidean divergence linked to the optimal nearest neighbor remains comparatively minimal, the discrepancy between the nearest neighbor methodology and the ANN's conservation projections is similarly narrow.

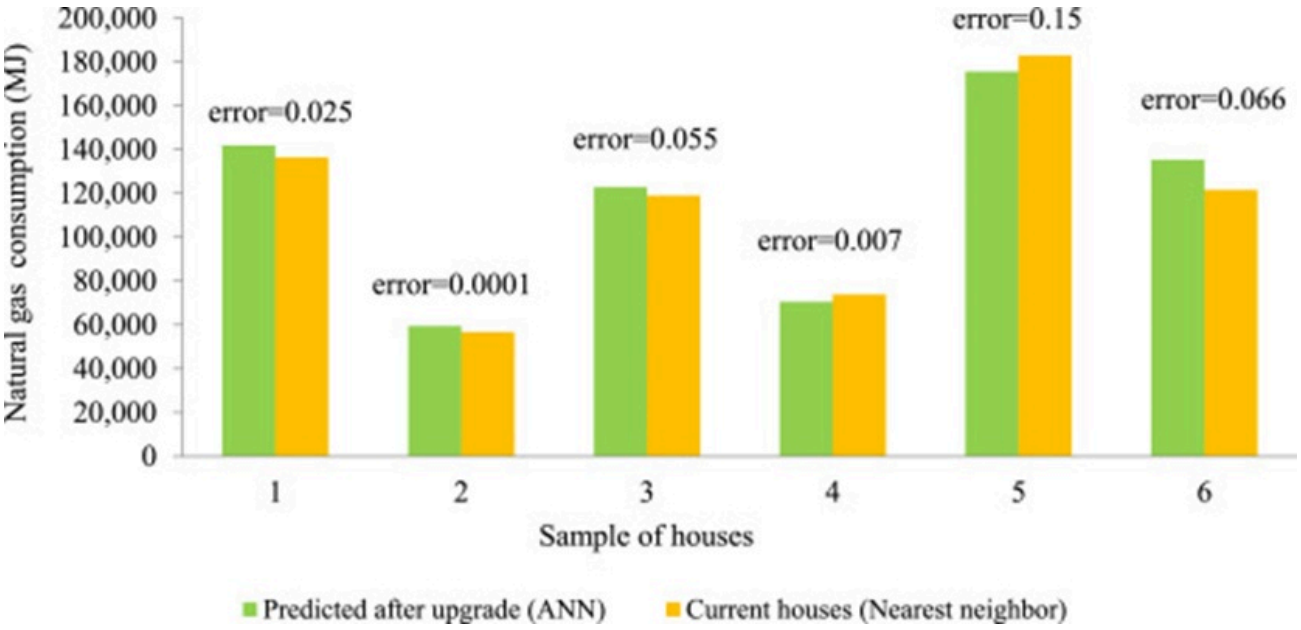

Figure 6. Comparison of predicted natural gas usage by ANN model with nearest neighbor method during winter season.

Results and Discussion

The outcomes derived from the implemented case analysis are delineated in this segment, reflecting the concluding phases of the established methodological architecture (i.e., steps 6–8).

Estimating individual and collective energy savings from efficiency upgrades (Step 6)

Once the predictive reliability regarding historical energy usage was confirmed, the calibrated neural network was subsequently applied to explore prospective conservation benefits stemming from targeted retrofits. This calibrated model facilitates such explorations by generating novel informational samples, rooted in empirical data sourced from properties that have already undergone thermal enhancements. **Table 7** details the specific interventions evaluated. These encompass the installation of wall and attic insulation, the integration of triple-paned window systems, water heater modernization (achieving an EF of 0.96), and furnace replacements (reaching 95% efficiency). The assigned thermal resistance parameters (R-values) for the wall and attic insulation enhancements stand at 2.28 and 7.04 m2K/W, respectively.

Table 7. The upgraded data used in ANN model construction.

Variable	Empty cell	Input

© 2026 The Author(s). | Published by Institute of Smart Energy Systems Press

R_{attic} (m^2K/W)		7.04
R_{window} (m^2K/W)		0.53
R_{wall} (m^2K/W)		2.28
Furnace efficiency, (%)		95%
Energy factor for water heater	Instant	0.96
	Storage	0.70
Heating slope, HS_{gas} (W/K)		Calculation
Heating balance point temperature (°C)		Calculation

Recognizing that the heating slope, HS_{gas}, and heating temperature balance point, $T_{bal,h}$, served as foundational inputs for defining energy usage profiles, and acknowledging that architectural renovations would alter these variables, it became imperative to project the post-retrofit shifts in these metrics. The adjustment to the heating slope was executed by noting that HSgas can be mathematically represented as:

$$HS_{gas} = \frac{sum\left(\frac{Ai}{Ri}\right)}{\eta_{fur}} \quad (4)$$

Where Ai is the envelope feature area (wall, window, or attic), Ri is the associated thermal resistance, and η_{fur} is the furnace efficiency. Should either the mechanical efficiency or the thermal resistance figures be modified, the resulting HSgas will correspondingly shift, as demonstrated within **Eq. 5.**

$$HS_{gas,current} - (((\frac{1}{R_{wall,current}}) - (\frac{1}{R_{wall,upgrade}})) * \left(\frac{Wall\ area}{\eta_{\mathrm{fur}}}\right)) \quad (5)$$

The structural heating temperature balance point, $T_{bal,h}$, is intrinsically linked to the heating slope to some degree. In scenarios characterized by an elevated heating slope, thermal dissipation from the dwelling becomes perceptible to occupants even at comparatively moderate external temperatures. Conversely, as efficiency interventions successfully suppress the heating slope, the corresponding temperature balance point will concurrently drop.

At this specific balance point threshold, the internal thermal gains of the dwelling are computed utilizing **Eq. 6**.

$$Q_{gains} = sum\left(\frac{Ai}{Ri}\right) * (T_i - T_{balh,gas}) \quad (6)$$

Following the execution of the efficacy upgrades, the revised $T_{balh,\ gas,\ upgrade}$ metric can be ascertained via **Eqs. 7–10**.

$$T_{balh,gas,upgrade} = T_i - \left(\frac{3.14 * E_{baseline,electric}}{HS_{gas,upgrade} * \eta_{\mathrm{fur}}}\right) \quad (7)$$

© 2026 The Author(s). | Published by Institute of Smart Energy Systems Press

$$T_{balh,gas,current} = T_i - \left(\frac{3.14 * E_{baseline,electric}}{HS_{gas,current} * \eta_{fur}} \right) \quad (8)$$

$$\Delta T_{balh,gas} = \left(\frac{3.14 * E_{baseline,electric}}{\eta_{fur}} \right) * \left(\left(\frac{1}{HS_{gas,current}} \right) - \left(\frac{1}{HS_{gas,upgrade}} \right) \right) \quad (9)$$

$$T_{balh,gas,upgrade} = T_{balh,gas,current} - \left(\left(\frac{3.14 * E_{baseline,electric}}{\eta_{fur}} \right) * \frac{1}{HS_{gas,current}} - \frac{1}{HS_{gas,upgrade}} \right) \quad (10)$$

Where T_i is the thermostat set-point temperature.

The parameterized data reflecting the renovated dwellings were subsequently processed through the established ANN architecture to evaluate valuable energy savings. The energy reductions yielded by specific residential retrofits are calculable via **Eq. 11.**

$$Savings = E_{total,\ current} - E_{total,\ improved} \quad (11)$$

Where $E_{total,\ current}$ and $E_{total,\ improved}$ are the total energy consumed for the current and improved house, respectively.

The prospective energy mitigation generated by deploying discrete EE strategies across a single winter cycle was estimated. The mean cold-season conservation metrics across the comprehensive residential dataset are presented in **Table 8**. As the findings explicitly demonstrate, the proportional natural gas reductions stemming from supplemental wall insulation vastly outperformed the benefits derived from both window modernizations and attic insulation additions, a disparity primarily driven by the fundamentally poor current state of insulation within the studied structures.

Table 8. Average natural gas savings from individual upgrades.

Parameter modified	Wall thermal resistance ((R_{wall}))	Attic thermal resistance ((R_{attic}))	Window thermal resistance ((R_{window}))	Furnace efficiency	Water heater energy factor
Mean natural gas savings	27,657 MJ	4,842 MJ	5,380 MJ	3,874 MJ	2,690 MJ
Mean percentage reduction in energy use	21.3%	3.7%	4.14%	2.95%	2.08%

Table 9 illustrates the prospective natural gas conservation attainable through the execution of aggregated EE interventions. The data indicate that enhancing the building envelope yields a more substantial impact than replacing water heaters and furnaces because existing mechanical systems are already reasonably efficient, and replacement

© 2026 The Author(s). | Published by Institute of Smart Energy Systems Press

costs exceed those of envelope enhancements. Consequently, these findings underscore the necessity for a more optimized, strategic EE enhancement framework, which is detailed in subsequent sections.

Table 9. Comparison of energy savings from different combinations of upgrading options.

Retrofit Scenario	Annual Energy Reduction	Energy Reduction (%)
Building envelope improvements only	33,253 MJ	25.62%
Building envelope improvements combined with furnace upgrade	34,760 MJ	26.82%
Building envelope, furnace, and water-heater upgrades combined	35,513 MJ	27.37%

Levelized cost of the adoption of energy efficiency measures (Step 7)

Leveraging the capacity to precisely project energy cost reductions across diverse EE interventions for all homes within the residential dataset, a tiered investment strategy was formulated. A levelized cost of savings indicator ($/MJ) was employed to establish this prioritization [37]. For these calculations, the operational lifespan of the investment was projected at 20 years for furnace and water heater modernizations, and 30 years for the remaining weatherization upgrades [38]. Additionally, the baseline fuel price and the yearly energy cost inflation rate were set at 0.6 $US/therm and 3%, respectively. To evaluate financial feasibility, a minimum attractive rate of return (MARR) of 7% was established as the baseline for project acceptability.

Table 10 presents the estimated expenditure for system enhancements, sourced from existing literature [31].

Table 10. Implementation cost of the EE measure.

Energy-efficiency upgrade measure	Cost per unit
Wall insulation enhancement	$7.9/m²
Attic insulation enhancement	$7.5/m²
Window replacement/upgrade	$226/m²
Heating system upgrade	$19/m²
Water-heating system upgrade	$19/m²

Levelized cost of fuel savings in all residences

Applying **Eqs. 1–6** alongside the projected energy conservation for each EE intervention, the levelized expenditures were computed individually for each dwelling. **Figure 7** illustrates the outcomes if all dwellings within the dataset received maximal-efficiency retrofits (indicated in green), contrasting these figures against the ‘break-even’ investment threshold established by McKinsey [37]. As depicted, solely the expenditure associated with wall insulation enhancements proved more advantageous than the McKinsey benchmark. This suggests that the proportional natural gas conservation derived from supplemental wall insulation substantially exceeded the savings generated by window modernizations or attic

© 2026 The Author(s). | Published by Institute of Smart Energy Systems Press

insulation installations. Furthermore, it demonstrates that indiscriminate capital allocation toward arbitrary EE interventions across the broader housing stock fails to yield financially viable cost-effectiveness.

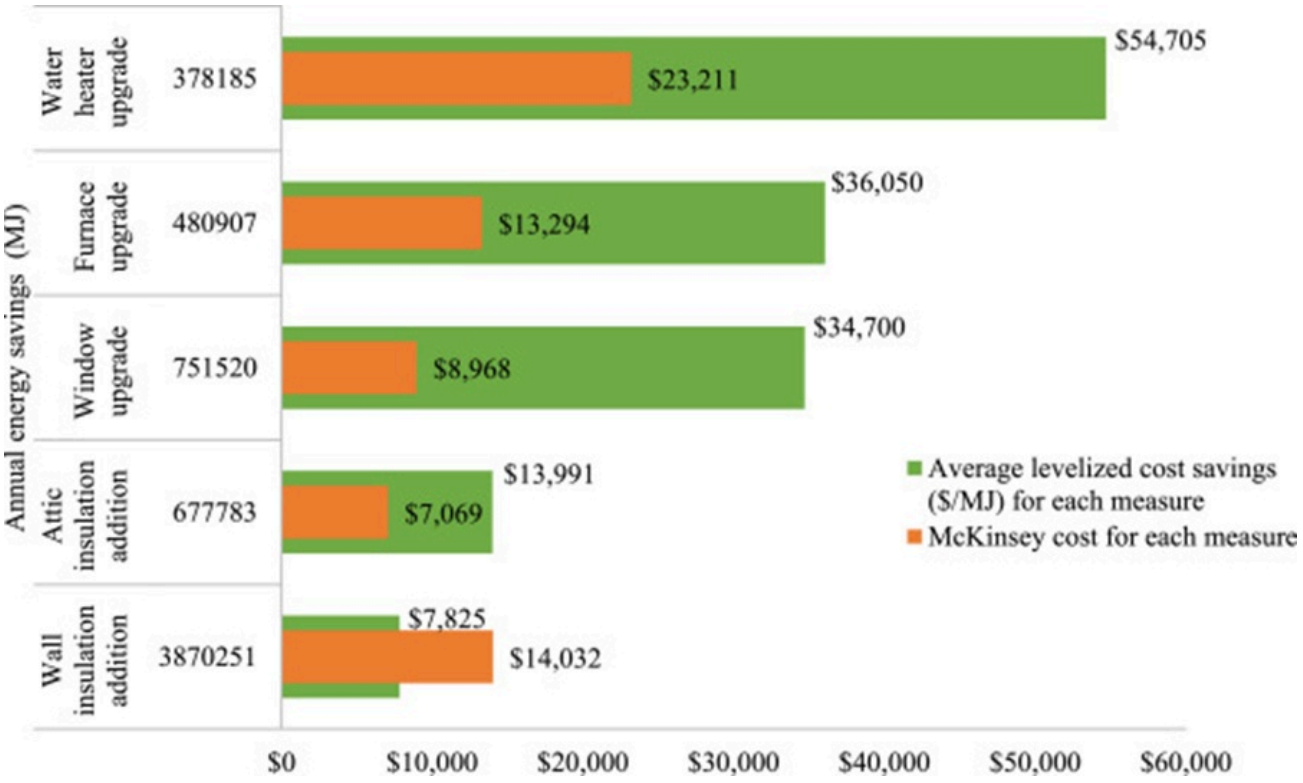

Figure 7. The annual energy savings for various measures vs. average levelized cost savings ($/MJ).

Individual levelized cost of prioritized investment

Figure 8 delineates the distribution density of the levelized cost of energy conservation across all homes for every evaluated efficiency strategy. These findings highlight the heterogeneous thermal performance characteristic of the analyzed housing inventory. The data reveal that the financial threshold to achieve savings via wall insulation upgrades represents the lowest among all evaluated conservation strategies. This underscores the significantly higher financial utility of prioritizing interventions with lower levelized costs.

© 2026 The Author(s). | Published by Institute of Smart Energy Systems Press

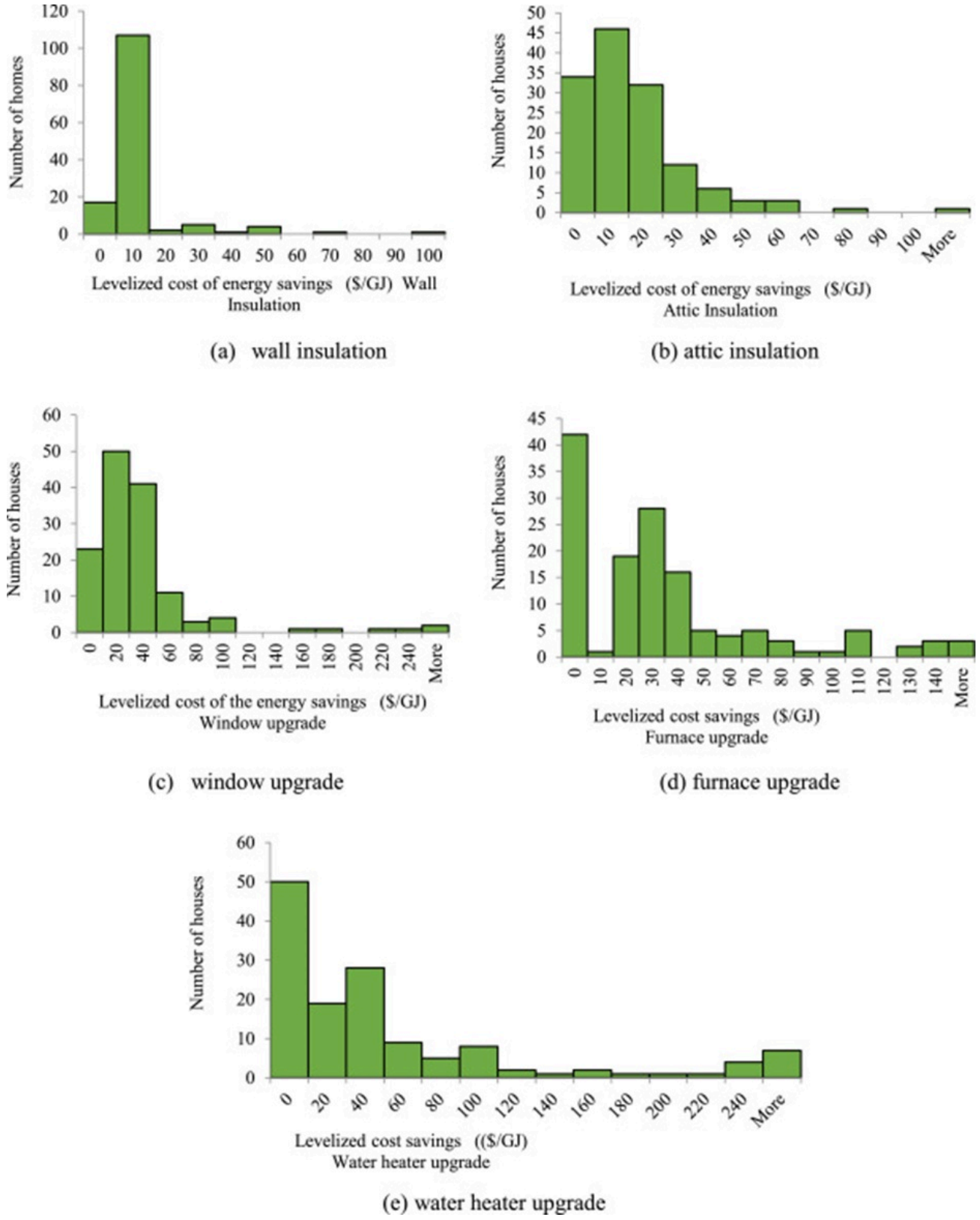

Figure 8. Histograms of levelized cost of energy savings ($/GJ).

Figure 9 provides an alternative viewpoint on the LCFS across the residential cohort, modeling a scenario where the intervention possessing the most favorable levelized cost is executed initially, followed sequentially by the next most

© 2026 The Author(s). | Published by Institute of Smart Energy Systems Press

economical option. The LCFS for every evaluated strategy is plotted in ascending progression relative to its economic efficiency. These outcomes explicitly demonstrate the financial prudence of establishing an investment hierarchy. The minimum LCFS figures for specific EE strategies fall beneath the established McKinsey benchmark. Additionally, the analysis reveals that particular investments harbor the capacity for broader implementation across the housing portfolio. To illustrate, fewer than 5% of the homes exhibit LCFS metrics for furnace and water heater upgrades that sit beneath the benchmark (a consequence of atypically elevated energy usage in those specific dwellings), whereas 78% present financially sound opportunities for wall insulation enhancements.

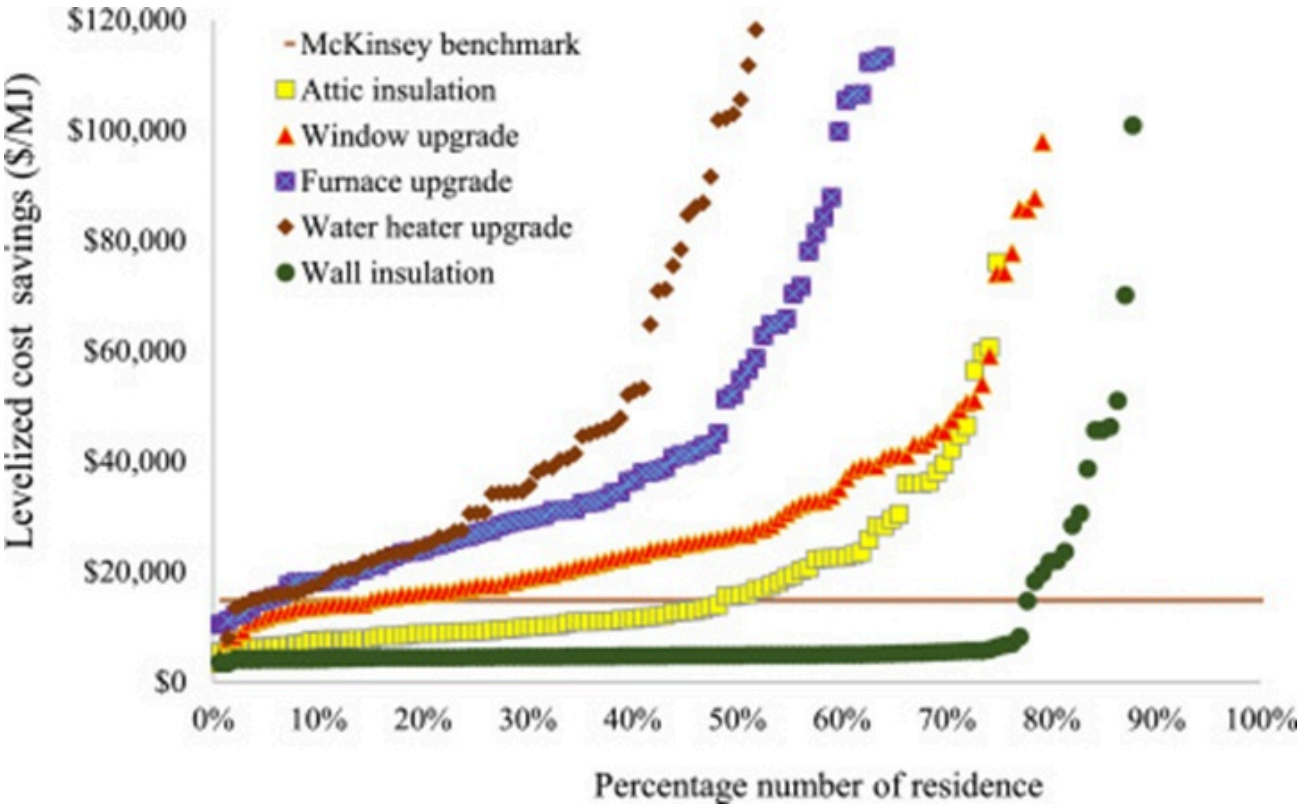

Figure 9. LCFS of EE measures for all residences (cost effectiveness shown in ascending order).

The cumulative levelized expenditure for deploying an EE intervention across k dwellings is defined in **Eq. 12.**

$$\text{Aggregate levelized cost of fuel savings}_j = \sum_{i=1}^{k} \frac{NPV_{i,j} + Initial\ cost_{i,j}}{Annual\ natural\ gas\ savings_{i,j}\ (\text{MJ}) \times Lifetime_j} \quad (12)$$

The implementation penetration rate of this specific intervention within the housing dataset, relative to these cumulative savings, is calculated as $k/N \times 100$, where N represents the aggregate count of homes.

Collective levelized cost of prioritized investment

While the preceding segment utilized a “worst-to-first” paradigm for isolated interventions, this portion investigates the phased integration of strategies across the comprehensive suite of measures to identify the most optimal LCFS. **Figure 10** displays the outcomes of this approach, plotting the cumulative LCFS against the proportional natural gas reductions. Executing a single EE enhancement generates a ripple effect that influences the efficacy of subsequent efficiency

© 2026 The Author(s). | Published by Institute of Smart Energy Systems Press

upgrades. For instance, while adding wall insulation immediately augments the structure's thermal performance, it simultaneously diminishes the prospective conservation yields of an independent furnace modernization, given that the improved envelope has already curtailed the baseline energy demand. **Figure 10** illustrates the feasibility of slashing energy consumption by 36% up to the benchmark LCFS limit of $14/mmBTU ($14,782/MJ) [37], underscoring the robust viability of this methodology.

Furthermore, it indicates that deeper energy reductions require substantially higher capital expenditures (reflected in the exponential segment of the curve). As an example, achieving a 38% drop in natural gas usage requires an investment of $20,115/MJ, while pushing for greater reductions mandates an exorbitant capital outlay that lacks financial justification. Consequently, the juncture where the LCFS trajectory shifts abruptly signifies the absolute threshold of cost-effective conservation achievable via present-day EE technologies.

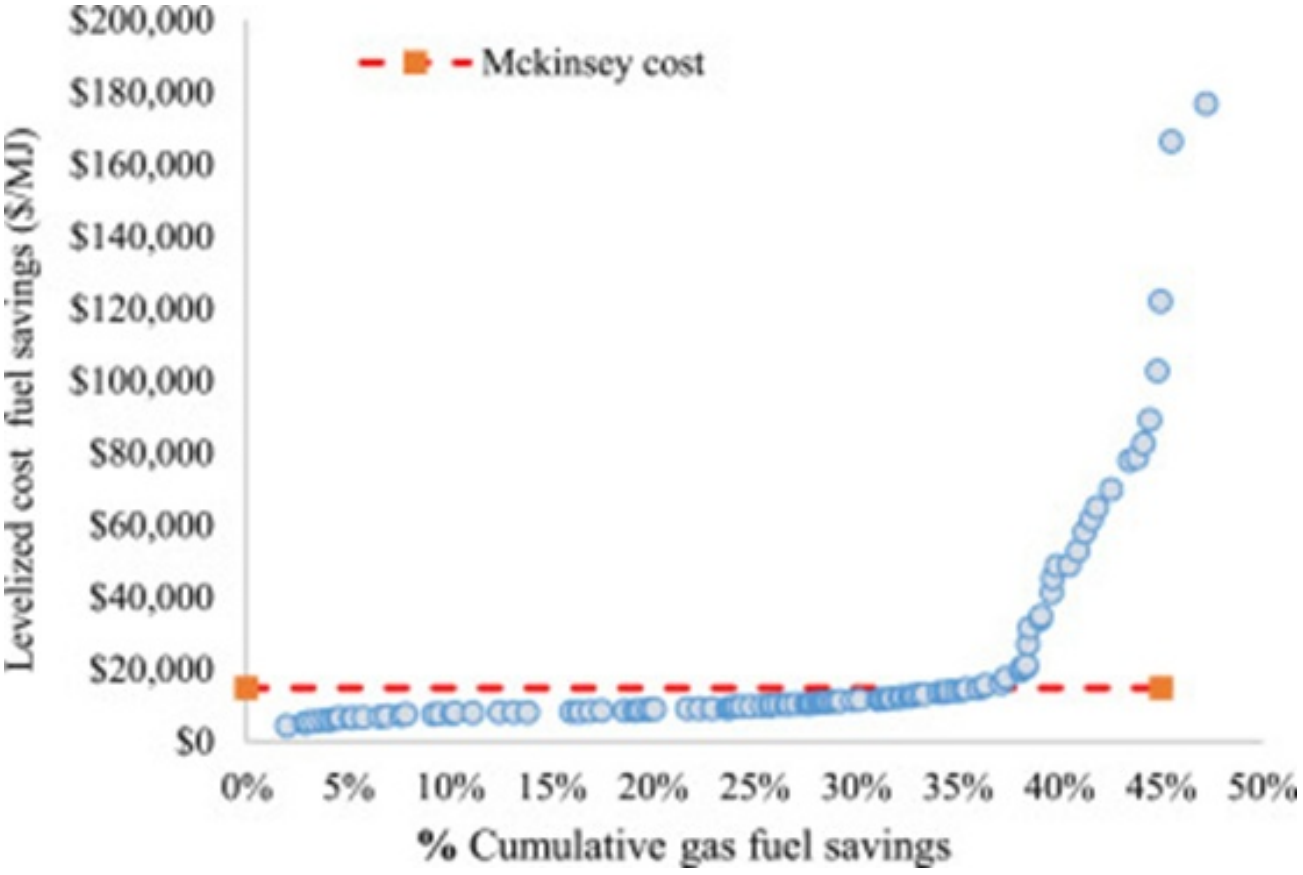

Figure 10. Aggregated LCFS for all houses as a function of percentage energy reduction.

Figure 11 demonstrates the pathways to attain varying magnitudes of energy conservation through the implementation of this "worst-to-first" methodology. As depicted, enhancements to wall insulation exerted the most profound influence on realizing targeted energy reductions. The data suggests that as the overall proportion of energy mitigated expanded, the absolute conservation derived from wall insulation enhancements grew concurrently. Conversely, the cumulative energy conservation generated by the remaining interventions was comparatively minor.

© 2026 The Author(s). | Published by Institute of Smart Energy Systems Press

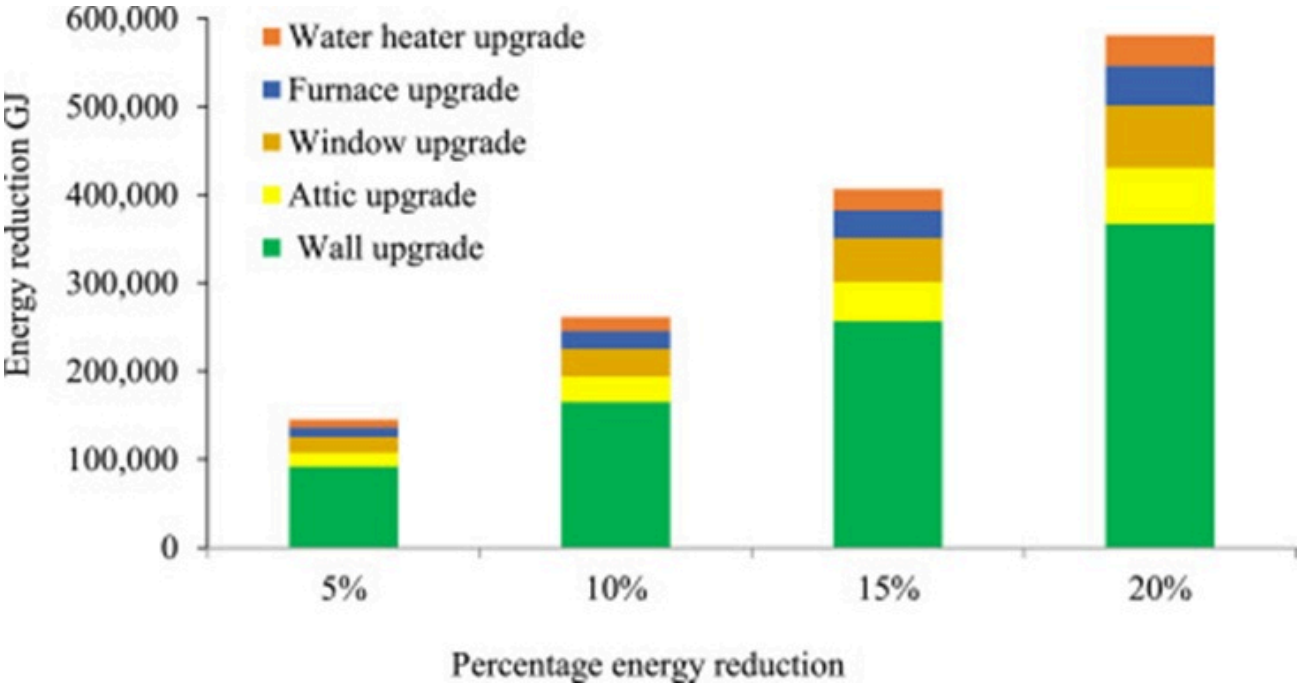

Figure 11. Scenarios for achieving various levels of energy reduction using "worst-to-first" approach.

Community-wide broader economic impact of EE (Step 8)

Table 11 presents the community-scale proportions of natural gas conservation, the yearly reduction in energy expenditures, and the requisite capital to subsidize each EE strategy evaluated within this research. Across all EE interventions, the break-even LCFS threshold of $14/mmBTU ($14,782/MJ) established by McKinsey serves as the benchmark for computing the percentile of natural gas conservation [37]. To illustrate, an aggregate 36% of natural gas usage can be mitigated while maintaining an LCFS beneath the $14/mmBTU ($14,782/MJ) limit across the evaluated measures.

Table 11. Savings and investment for achieving LCOS $14/mmBTU ($14,782/MJ) from EE measures.

Retrofit option	Share of natural gas reduction	Yearly monetary savings ($)	Capital investment ($)
Wall insulation retrofit	0.48	16,024	117,967
Attic insulation retrofit	0.35	4,647	83,514
Window retrofit	0.10	2,707	59,703
Furnace replacement	0.10	1,846	26,928
Water-heater replacement	0.10	1,806	27,111

To quantify the ripple effects on the local economy, this investigation merged an economic input–output (EIO) architecture with granular municipal datasets. EIO analysis systematically delineates the direct, indirect, and induced economic consequences of capital allocations across a broader market. For instance, a drive to augment residential EE inherently boosts the manufacturing output of industries producing those efficiency materials; this constitutes the direct impact. This

© 2026 The Author(s). | Published by Institute of Smart Energy Systems Press

initial capital injection subsequently stimulates elevated output among ancillary suppliers delivering necessary raw materials and logistical services (representing the indirect impact). This surge in both primary and secondary production frequently translates into new employment opportunities or higher wages. Subsequently, this expansion in household disposable income is often recirculated within the municipality through expenditures on recreation, education, and various local services (encapsulating the induced impact).

While a comprehensive theoretical breakdown of the IO paradigm falls outside the purview of this paper, the Leontief IO model [39] functions as the foundational architecture for this analysis. The Leontief framework treats fluctuations in final demand as exogenous variables, computing the necessary adjustments in gross industrial output to maintain equilibrium between supply and demand across all market sectors. A primary premise of the classical Leontief structure is the static direct requirement matrix A, which denotes the fractional monetary input a specific sector demands to generate a single dollar of market output. Stated differently, these input coefficients signify the monetary contributions from sector i essential to yield $1 of production in sector j, based upon the established financial transaction matrix. This matrix is customarily deployed to evaluate shifts in the aggregate production vector (x) triggered by alterations in the final demand vector (y), as modeled in **Eq. 13:**

$$\Delta x = (\mathbf{I} - \mathbf{A})^{-1} \Delta y \quad (13)$$

Where A constitutes the n × n direct requirement matrix, y represents the financial valuation of the final demand column vector, x is the aggregate monetary industrial production column vector, and v functions as the monetary value-added row vector. **Table 12** catalogs the ten industrial domains within Montgomery County, OH (the locale of the evaluated properties) that have garnered the most significant economic benefits from residential wall insulation capital allocations. While the leading three sectors experienced direct surges in commercial transactions and service demands stemming from these capital injections, the remaining industries were similarly stimulated via indirect and induced economic pathways. The former—indirect or supply-chain repercussions—are primarily linked to vendors supplying base materials to those top three sectors; notably, these impacts appear relatively muted within the local municipality, implying that a majority of essential manufacturing components are sourced externally.

Table 12. Top 10 industries impacted by local wall insulation investment.

Economic sector / Industry category	Economic output
Architecture, engineering, and associated professional services	$60,882
Manufacturing of fiberglass insulation materials	$29,495
Production of thermal insulation and polystyrene foam products	$29,493
Imputed rental services for owner-occupied residential properties	$5,462
Food service establishments and beverage providers	$3,943
Private healthcare and hospital services	$3,317
Real estate service providers and establishments	$3,211
Central banking, monetary authorities, and deposit-based credit intermediation	$2,707
Wholesale trade sector	$2,657
Telecommunications services	$2,637
Additional 430+ industrial sectors	—

© 2026 The Author(s). | Published by Institute of Smart Energy Systems Press

As demonstrated by the other seven industrial categories, the compounding financial influence of wall insulation expenditures inherently encompasses induced economic activity. For example, personnel employed at insulation manufacturing plants might inject their augmented earnings—derived from the heightened demand for EE materials—back into the local ecosystem via residential leasing, healthcare utilization, and increased consumption of food and beverages. An identical analytical protocol was applied to the remaining EE strategies, with **Figure 12** detailing the proportional distribution of direct, indirect, and induced community-level economic consequences linked to each investment.

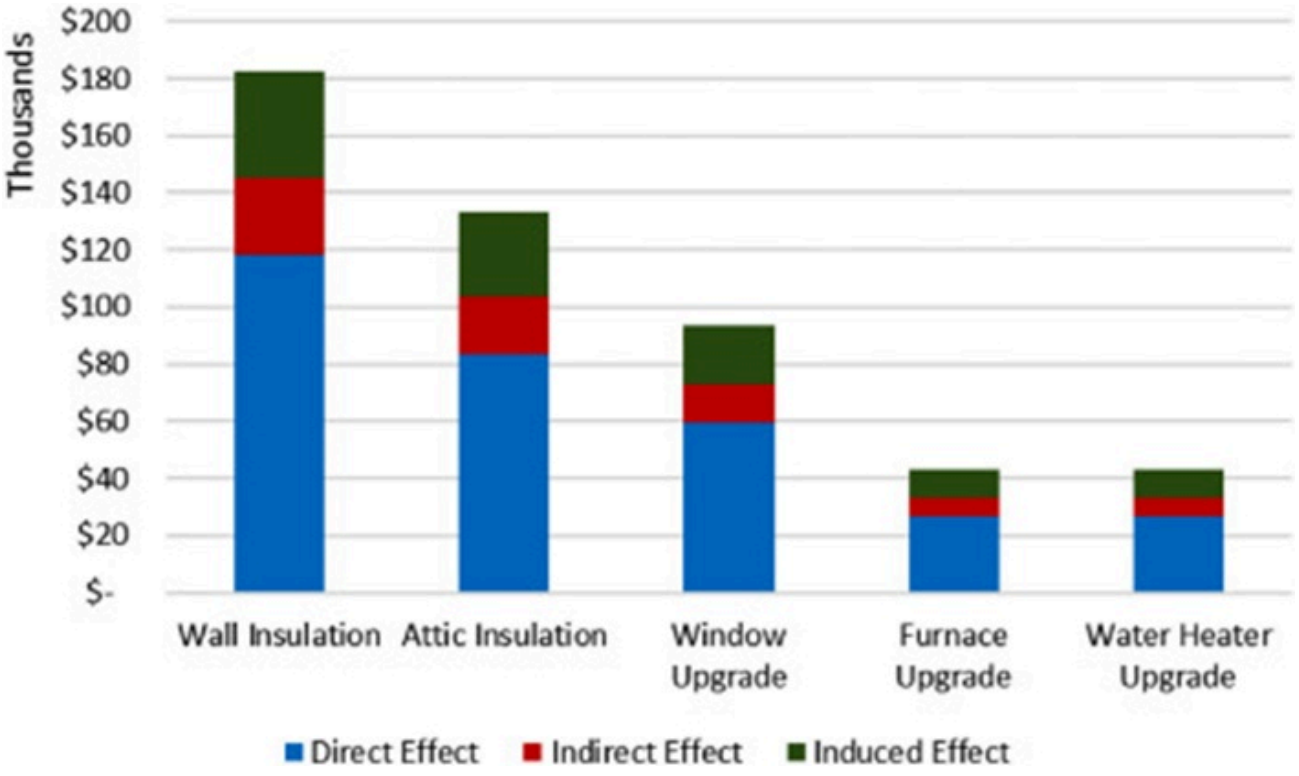

Figure 12. Breakdown of local economic impact by EE investment.

Table 13 summarizes these compounding economic repercussions.

Table 13. Economic impacts of EE installation to the community.

Economic indicator	Wall insulation	Attic insulation	Window upgrade	Furnace upgrade	Water heater Upgrade	Total value
Direct effect contribution	$117,968	$83,515	$59,704	$26,928	$26,928	$315,043
Indirect effect contribution	$27,078	$20,105	$13,117	$6,093	$6,093	$72,486
Induced effect contribution	$37,737	$29,560	$20,806	$10,122	$10,122	$108,347
First-year monetary savings	$16,024	$4,647	$2,707	$1,846	$1,846	$27,070
Ten-year cumulative monetary savings	$160,235	$46,465	$27,068	$18,462	$18,462	$270,692

© 2026 The Author(s). | Published by Institute of Smart Energy Systems Press

The profound relevance of these findings becomes particularly clear when projecting the data across the City of Dayton, which contains slightly more than 45,000 single-family dwellings structurally analogous to the evaluated sample. To realize the designated 36% contraction in energy usage, an upfront EE capital allocation of $26.1M would be necessitated; however, the subsequent compounded economic ripple effect would generate an estimated $41.2M. Furthermore, the retained capital resulting from these thermal efficiency upgrades would stimulate a supplementary economic impact totaling $2.21M over the operational lifespan of the implemented strategies.

Conclusion

The advanced methodological framework seeks to isolate the most financially viable energy conservation interventions, facilitating their phased implementation while prioritizing strategies that utilize accessible—or ascertainable—structural and energetic metrics across a broad portfolio of single-family dwellings. An ANN architecture is deployed to project natural gas conservation alongside the levelized expenditures for a wide array of potential structural efficiency upgrades. Empirical machine learning forecasting systems have traditionally relied on easily procured datasets, encompassing variables such as meteorological records, resident occupancy rates, and sociodemographic profiles. Few antecedent studies have integrated granular structural properties, primarily due to the logistical hurdles of acquiring such data at a macro (regional) scale. The formulated analytical architecture permits the projection of both baseline energy utilization and the prospective conservation attainable through the execution of discrete EE interventions. This model operates using a constrained array of verifiable architectural parameters—including geometric dimensions and thermal traits—coupled with empirical energy usage and longitudinal meteorological records. The informational inputs necessitated by this approach are substantially less voluminous than those mandated by comprehensive, physics-driven energy simulations. The outcomes demonstrate the feasibility of precisely deploying the trained neural network to forecast conservation yields from targeted efficiency enhancements, validated against the projected usage of a localized residential sub-sample. Considering that the majority of municipalities in the US Midwest feature housing stocks exhibiting thermal variance akin to the evaluated sample—which realized a 36% efficiency gain at an LCFS beneath $14/mmBTU ($14,782/MJ)—the deployment of a “worst-to-first” mitigation framework demonstrates a profound capacity for substantial regional impact. For municipal planners and policymakers, these findings can serve as a foundational blueprint for formulating broader urban energy conservation directives. The robust conservation projections introduced in this study can instill greater certainty within financial decision-making paradigms regarding EE capital allocations. Although the granular data required to calibrate the proposed machine learning architectures is not currently in the public domain, significant potential exists to systematically aggregate this information via standard municipal property appraisals and routine residential inspections. Moreover, the exact analytical framework detailed in this investigation can be adapted to structure and prioritize future capital investments targeting the integration of renewable energy systems.

Acknowledgements

None

Conflict of interest

None

Financial support

© 2026 The Author(s). | Published by Institute of Smart Energy Systems Press

None

Ethics statement

None

Received: 27 Jul 2024 Revised: 01 Oct 2024 Accepted: 18 Oct 2024
Published online: 15 June 2026

Rights and permissions

Open Access The author(s) retain copyright. This article is licensed under the Creative Commons Attribution-NonCommercial-ShareAlike 4.0 International License. It may be shared and adapted for non-commercial purposes with appropriate attribution, an indication of changes, and distribution of adaptations under the same license. Third-party material may be subject to separate terms identified in its credit line. View the license at https://creativecommons.org/licenses/by-nc-sa/4.0/.

References

1. Energy Information Administration (EIA). Residential Energy Consumption Survey (RECS). Washington, DC: Energy Information Administration; 2016.
2. Hagerman J. Building America kick-off. Washington, DC: US Department of Energy - Energy Efficiency & Renewable Energy; 2010.
3. Reinhart CF, Cerezo Davila C. Urban building energy modeling – a review of a nascent field. Build Environ. 2016;97:196-202.
4. Bourdic L, Salat S. Building energy models and assessment systems at the district and city scales: a review. Build Res Inf. 2012;40(4):518-26.
5. Bucking S, Dermardiros V. Distributed evolutionary algorithm for co-optimization of building and district systems for early community energy masterplanning. Appl Soft Comput. 2018;63:14-22.
6. Kammen DM, Sunter DA. City-integrated renewable energy for urban sustainability. Science. 2016;352(6288):922-8.
7. Srebric J, Heidarinejad M, Liu J. Building neighborhood emerging properties and their impacts on multi-scale modeling of building energy and airflows. Build Environ. 2015;91:246-62.
8. Koo C, Hong T, Oh J, Choi JK. Improving the prediction performance of the finite element model for estimating the technical performance of the distributed generation of solar power system in a building façade. Appl Energy. 2018;215:41-53.
9. Kang H, Lee M, Hong T, Choi JK. Determining the optimal occupancy density for reducing the energy consumption of public office buildings: a statistical approach. Build Environ. 2018;127:173-86.
10. Alanne K, Cao S. Zero-energy hydrogen economy (ZEH2E) for buildings and communities including personal mobility. Renew Sustain Energy Rev. 2017;71:697-711.
11. Barbiero T, Grillenzoni C. A statistical analysis of the energy effectiveness of building refurbishment. Renew Sustain Energy Rev. 2019;114:109297.

12. Klein SJW, Coffey S. Building a sustainable energy future, one community at a time. Renew Sustain Energy Rev. 2016;60:867-80.

13. Liu Z, Zhou Q, Tian Z, He BJ, Jin G. A comprehensive analysis on definitions, development, and policies of nearly zero energy buildings in China. Renew Sustain Energy Rev. 2019;114:109314.

14. Choi JK, Eom J, McClory E. Economic and environmental impacts of local utility-delivered industrial energy-efficiency rebate programs. Energy Policy. 2018;123:289-98.

15. Rastogi A, Choi JK, Hong T, Lee M. Impact of different LEED versions for green building certification and energy efficiency rating system: a multifamily midrise case study. Appl Energy. 2017;205:732-40.

16. Gillingham K, Newell R, Palmer K. Energy efficiency policies: a retrospective examination. Annu Rev Environ Resour. 2006;31:161-92.

17. Koomey JG, Martin NC, Brown M, Price LK, Levine MD. Costs of reducing carbon emissions: US building sector scenarios. Energy Policy. 1998;26(5):433-40.

18. Ahmad T, Chen H, Guo Y, Wang J. A comprehensive overview on the data driven and large scale based approaches for forecasting of building energy demand: a review. Energy Build. 2018;165:301-20.

19. Amara F, Agbossou K, Dubé Y, Kelouwani S, Cardenas A, Bouchard J. Household electricity demand forecasting using adaptive conditional density estimation. Energy Build. 2017;156:271-80.

20. González-Vidal A, Jiménez F, Gómez-Skarmeta AF. A methodology for energy multivariate time series forecasting in smart buildings based on feature selection. Energy Build. 2019;196:71-82.

21. Chen Y, Wu J. Distribution patterns of energy consumed in classified public buildings through the data mining process. Appl Energy. 2018;226:240-51.

22. Fan C, Xiao F, Wang S. Development of prediction models for next-day building energy consumption and peak power demand using data mining techniques. Appl Energy. 2014;127:1-10.

23. Karatasou S, Santamouris VG. Modeling and predicting building's energy use with artificial neural networks: methods and results. Energy Build. 2006;38:949-58.

24. Chae YT, Horesh R, Hwang Y, Lee YM. Artificial neural network model for forecasting sub-hourly electricity usage in commercial buildings. Energy Build. 2016;111:184-94.

25. Kang Y, Krarti M. Bayesian-emulator based parameter identification for calibrating energy models for existing buildings. In: Building Simulation. Springer; 2016.

26. González-Vidal A, Moreno-Cano V, Terroso-Sáenz F, Skarmeta AF. Towards energy efficiency smart buildings models based on intelligent data analytics. Procedia Comput Sci. 2016;83:994-9.

27. Singaravel S, Geyer P, Suykens J. Deep neural network architectures for component-based machine learning model in building energy predictions. In: eg-ice Workshop; 2017.

28. Chonan Y, Nishida K, Matsumoto T. Great energy predictor shootout II – a Bayesian nonlinear regression with multiple hyperparameters. In: Proceedings of the 1996 Annual Meeting of the American Society of Heating, Refrigerating and Air-Conditioning Engineers; 1996; San Antonio.

29. Aqlan F, Ahmed A, Srihari K, Khasawneh MT. Integrating artificial neural networks and cluster analysis to assess energy efficiency of buildings. In: Proceedings of the 2014 Industrial and Systems Engineering Research Conference; 2014; Canada.

© 2026 The Author(s). | Published by Institute of Smart Energy Systems Press

30. Sadineni SB, France TM, Boehm RF. Economic feasibility of energy efficiency measures in residential buildings. Renew Energy. 2011;36:2925-31.

31. Villoria-Siegert R, Brodrick P, Hallinan KP, Brecha R. Cost-availability curves for hierarchical implementation of residential energy-efficiency measures. Energy Effic. 2014;8(2):267-79.

32. Choi JK, Morrison D, Hallinan KP, Brecha RJ. Economic and environmental impacts of community-based residential building energy efficiency investment. Energy. 2014;78:877-86.

33. Breiman L. Random Forests. Mach Learn. 2001;45(1):5-32.

34. Fels M. PRISM: an introduction. Energy Build. 1986;9(1-2):5-18.

35. Yalcintas M, Akkurt S. Artificial neural networks applications in building energy predictions and a case study for tropical climates. Int J Energy Res. 2005;29(10):891-901.

36. Multivariate k-nearest neighbour regression for time series data – a novel algorithm for forecasting UK electricity demand. In: Proceedings of the 2013 International Joint Conference on Neural Networks (IJCNN); 2013.

37. Granade HC, Creyts J, Derkach A, Farese P, Nyquist S, Ostrowski K. Unlocking energy efficiency in the US economy. McKinsey Global Energy and Materials; 2009.

38. US Environmental Protection Agency (EPA). ENERGY STAR – energy efficient products. Washington, DC: United States Environmental Protection Agency; 2017.

39. Choi JK, Bakshi BR, Hubacek K, Nader J. A sequential input–output framework to analyze the economic and environmental implications of energy policies: gas taxes and fuel subsidies. Appl Energy. 2016;184:830-9.

© 2026 The Author(s). | Published by Institute of Smart Energy Systems Press